MNRAS 000, 1–?? (2015) Preprint 27 April 2016 Compiled using MNRAS LATEX style file v3.0

Generating potassium abundance variations in the Solar Nebula

Alexander Hubbard,[1]⋆
[1]Department of Astrophysics, American Museum of Natural History, New York, NY 10024-5192, USA

Accepted XXX. Received YYY; in original form ZZZ

arXiv:1604.07727v1 [astro-ph.EP] 26 Apr 2016

ABSTRACT

An intriguing aspect of chondritic meteorites is that they are complementary: while their separate components have wildly varying abundances, bulk chondrites have nearly solar composition. This implies that the nearly-solar reservoirs in which chondrites were born were in turn assembled from sub-reservoirs of differing compositions that birthed the different components. We focus on explaining the potassium abundance variations between chondrules even within a single chondrite, while maintaining the observed CI ^{41}K to ^{39}K ratios. This requires physically separating potassium and chondrules while the temperature is high enough for K to be in the gas phase. We examine several mechanisms which could drive the dust through gas and show that to do so locally would have required long (sub-orbital to many orbits) time scales; with shortest potassium depletion time scales occurring in a scenario where chondrules formed high above the midplane and settled out of the evaporated potassium. While orbital time scales are at odds with laboratory chondrule cooling rate estimates, any other model for the origin for the potassium abundance variation has to wrestle with the severe logistical difficulty of generating a plethora of correlated reservoirs which varied strongly in their potassium abundances, but not in their potassium isotope ratios.

Key words: hydrodynamics – turbulence – meteorites, meteors, meteoroids – planets and satellites: composition – planets and satellites: formation – protoplanetary discs

1 INTRODUCTION

Of all the planetary systems known, our own is the only one where we have detailed elemental and isotopic data for any solid body. The dominant story told by that data is that, excluding objects with exceptionally traumatic histories (e.g. Mercury and the Moon), and focusing on the more refractory elements, solid objects throughout the solar system have loosely comparable bulk abundances (Palme 2000). This is not surprising as protoplanetary disks are expected to be quite active, and hence well mixed (Shakura & Sunyaev 1973; Lynden-Bell & Pringle 1974). Indeed, even if there is a magnetic dead zone (Gammie 1996; Bai 2014), turbulence from surface layers can penetrate and mix an otherwise quiescent midplane (Oishi & Mac Low 2009). Further, macroscopic solids in the solar nebula were made of vast numbers of sub-micron interstellar grains, erasing any stochastic compositional variations between said grains (Draine 2003).

However, when examined in finer detail there are significant variations which point to the solar nebula having contained separate reservoirs with different abundances from which different classes of solids were formed (McDonough 2003). In particular for this paper, different chondrite classes have modestly different abundances (Weisberg et al. 2006). Because chondrites are undifferentiated, and sometimes only slightly thermally or aqueously altered, meteorites, they provide an accessible record of the chemical and isotopic environments in which they and their components formed (Van Schmus & Wood 1967).

There is growing evidence for complementarity: chondrite components with strongly varying compositions combine to form chondrites with overall solar bulk composition (Hezel & Palme 2010; Palme et al. 2015). This implies that distinctly different parts of a chondrite, such as its chondrules and its matrix, were correlated with one another. While complementarity between chondrules and matrix can be maintained in the face of turbulent mixing for thousands of orbits assuming that the matrix and chondrules originated from a single reservoir, it cannot be produced after the fact by fortuitous radial transport (Goldberg et al. 2015). Complementarity therefore implies that the separate larger scale reservoirs with mostly solar bulk composition from which the different chondrite classes were assembled were, themselves, either divided into or assembled from smaller scale reservoirs with quite different, strongly non-solar, compositions. In particular for this work, potassium abundances vary by factors of many between different chondrules even within a given chondrite (Hewins 1991).

As noted above, the sets of small scale reservoirs implied by meteoritic components of differing compositions were correlated as is implied by complementarity. If they were not themselves drawn in some fashion from initial overarching large scale reservoirs of nearly solar composition which were preserved by the chondrite assemblage process, then their very existence across multiple chondrite classes would require an awkward degree of fine tuning. As

⋆ E-mail: ahubbard@amnh.org

© 2015 The Authors

we will develop in greater detail, the differing potassium abundances imply the existence of small scale reservoirs which were alternately strongly depleted of, and weakly enriched in K. In this paper we examine the conditions, and crucially the time scales, required for splitting an initially solar abundance reservoir into sub-reservoirs with differing potassium abundances. The results are generalizable and can be used to understand the lack of potassium isotope signatures throughout the Solar System, even between objects with wildly varying bulk potassium abundances (Humayun & Clayton 1995). The calculations further apply for generating any condensation temperature dependent depletions during planet formation although the temperature histories implied would differ.

2 CHONDRULES AND CHONDRITES

Chondrites are a set of classes of undifferentiated meteorites composed of a mix of chondrules, matrix, and other inclusions including Ca-, Al-rich inclusions (CAIs) (Weisberg et al. 2006). Chondrules are sub-mm glassy clasts which were produced by melting dust in the solar nebula, the protoplanetary disk in which our Solar System formed (Hewins 1997). While the mechanism through which chondrules were made is as yet uncertain, the melting required temperatures above 1700 K (Hewins & Radomsky 1990). Much of the space between chondrules is filled with fine-grained matrix material which was not heated to such a degree. Indeed, evidence suggests that only a small fraction of the matrix material could have been heated above 700 K (Huss & Lewis 1995; Mendybaev et al. 2002) which means that models for chondrule and chondrite formation must allow for solids that experienced very different thermal histories to have ended up in close proximity (Hubbard & Ebel 2015).

Researchers have amassed a range of evidences arguing that different classes of chondrites sampled different chondrule or chondrule precursor reservoirs (Jones 2012). These include differences in oxygen isotope ratios, bulk compositions, chondrule sizes, abundances of relic grains, and chondrule textural types. While taken individually, these lines of evidence are not conclusive but combined they are persuasive enough that in this paper we assume that different chondrite classes did indeed form from distinct reservoirs. Note however that these distinct reservoirs could have had identical bulk abundances and have differed primarily how in the chondrules were processed or how the chondrites were assembled: what matters for this paper is merely the logistical difficulty of generating a multitude of large scale reservoirs which in turn contain a large number of correlated small scale reservoirs.

Among the classification schemes used for chondrules is one that depends on their olivine fayalite (Fe_2SiO_4) fraction: the more common Type I chondrules have less than 10 mol % fayalitic olivine while the rarer Type II chondrules have Fa $>$ 10 mol % (McSween 1977a,b). A further difference between the two types of chondrules is their moderate volatile content: Type I chondrules are strongly depleted in moderately volatile elements such as sodium and potassium, while Type II chondrules are weakly enriched in those same elements (McSween 1977a,b; Jones & Scott 1989; Jones 1990). This potassium abundance difference will be our focus.

3 NEED FOR SUB-RESERVOIRS

Potassium is moderately volatile, with a 50% condensation temperature of approximately 1000 K under nebular conditions (Lodders 2003). That is far lower than the chondrule melting temperature of 1700 K, so it is reasonable to imagine that differing thermal histories acting on two separate regions of the solar nebula with identical bulk compositions led to the potassium depletion seen in Type I chondrules. In this paper we will show that the time scales required for such processes are not insignificant.

Importantly, potassium has two abundant stable isotopes, ^{39}K and ^{41}K. Therefore, straightforward partial evaporation would Rayleigh fractionate those isotopes by preferentially evaporating the lighter ^{39}K, leaving a heavy isotopic signature. Neither heavy, nor indeed light, isotopic signatures have been found in chondrules for potassium, or for iron either (Alexander et al. 2000; Alexander & Wang 2001). There are several broad categories of processes which could explain the differing elemental abundances without leaving behind an isotopic signature.

Firstly, there are processes where the gas and dust were out of isotopic and elemental equilibrium with each other when cooling through the potassium condensation temperatures. In such cases Raleigh fractionation was unavoidable when and where condensation occurred, but only to the degree said condensation actually occurred. For Type I chondrules, that means that they either formed from reservoirs which were tuned to result in both the observed elemental (potassium depleted with respect to CI) and isotopic (not potassium fractionated with respect to CI) abundances, or that their chondrule melting process must have been too short for meaningful evaporation and recondensation to have taken place. Given the spread in the chemical signatures seen across chondrules, it is implausible that so many different initial reservoirs existed whose elemental and isotopic abundances were carefully tuned such that their isotopic compositions converged upon melting, evaporation and recondensation (Hewins 1991; Humayun & Clayton 1995).

If on the other hand the heating and cooling associated with chondrule formation was so fast that no evaporation (and subsequent recondensation) occurred, then chondrules explicitly preserve the composition of their precursors. In that case Type I and II chondrules still had to have sampled different reservoirs, but the reservoirs would have only differed in their elemental, but not isotopic, abundances. In this case, the heating and cooling would have had to have been extremely fast: more than 10000 K/hr (Yu & Hewins 1997; Alexander et al. 2000; Alexander 2004), while current models for chondrule formation struggle to reach even 5000 K/hr (Boley et al. 2013). Further, experimental work has established that such cooling rates are too hight to be consistent with the crystallization textures of most chondrules (Desch et al. 2012, and references therein).

Secondly, the gas and dust could have been in equilibrium during at least the cooling phase of chondrule formation, in which case there would be no isotopic signature as long as the total system never developed one (Davis et al. 2005; Alexander et al. 2008). In equilibrium, as condensation occurs solids reabsorb evaporated species; so different equilibrium solid abundances require different system abundances during cooling. This case therefore requires reservoirs which differed in their elemental, but not isotopic, abundances. We divide this case into two: either equilibrium was maintained by not having evaporation and recondensation occur, or it was maintained by having a sufficiently slow process. It would have been possible to avoid evaporation and recondensation if the ambient gas had maintained exactly the correct amount of potas-

sium (perhaps by moving through a planetesimal atmosphere Morris et al. 2012) to match the correct vapor pressure to avoid evaporation and condensation over the thermal history of a given chondrule and for a range of observed potassium depletion patterns in chondrules. That scenario does not seem plausible. It would more naturally arise if the solids were so concentrated that only a negligible degree of K evaporation was needed to reach equilibrium K vapor pressures.

Such large (factors of more than 100) increases in the dust concentration are difficult to achieve, especially for chondrule precursors which were presumably porous and therefore at least as well coupled to the gas as chondrules (Jacquet et al. 2012). While turbulence can preferentially concentrate same-sized dust grains (Cuzzi et al. 2001), this requires narrow dust size distributions (Hubbard 2013). The meteoritic record shows modest but still significant scatter in chondrule sizes even within a given meteorite (Friedrich et al. 2015), so large turbulent dust concentrations are not expected to have occurred. Worse, at the size and densities invoked the dust clouds would have been gravitationally unstable (Alexander et al. 2008), and gravitational collapse occurs quickly, on orbital time scales (Johansen et al. 2009). If the chondrule formation mechanism did not itself generate such dust concentrations, it would require excessive fine tuning for chondrule melting events to have occurred only just before gravitational collapse at a rate sufficient to explain chondrules, while leaving the matrix untouched. Shock models for chondrule melting do concentrate the dust, but only by factors of order ten (Morris et al. 2012); and even if such a coincidence of chondrule heating and dust concentration occurred, it is difficult to imagine how the matrix, which was not heated and makes up a significant fraction of even the ordinary chondrites, could have been evenly mixed in during the gravitational collapse stage of planetesimal formation (Hubbard & Ebel 2015).

In the cases of both rapid heating and cooling and extreme solid enrichment the initial dust composition matches the final dust composition, so the origin of the reservoirs cannot be due to the chondrule formation process itself. This merely pushes the origin of the Type I and II chondrule potassium difference back in time, and raises the question of how different reservoirs with identical isotopic but different elemental abundances could have been generated without invoking evaporation and condensation. If the elemental composition differences were inherited from pre-solar gas, the lack of an isotopic signature would be quite surprising; but any evaporation and recondensation of K in the solar nebula would have required temperatures on the order of 1000 K, high enough to have thermally processed matrix material. That has been ruled out by laboratory analysis (Huss & Lewis 1995; Mendybaev et al. 2002).

Finally, we are left with the gas and dust having cooled slowly through the condensation temperatures. If they cooled slowly enough, isotopic equilibrium would have been maintained. Further, local processes would have had time to split the large scale reservoir from which a given chondrite was assembled into sub-reservoirs with differing total system (gas plus solids) potassium abundances. In this case the chondrule formation process itself would generate the different potassium elemental abundances without raising isotopic questions, greatly simplifying the logistical difficulties associated with generating many reservoirs with varying elemental abundances.

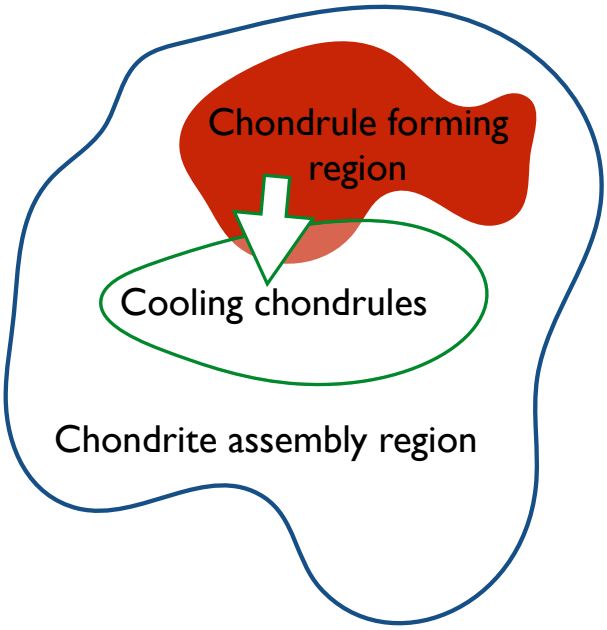

Figure 1. Cartoon of how sub-reservoirs are generated within a larger chondrite assembly reservoir. The overarching reservoir maintains complementarity. Chondrules move out of the chondrule forming region sufficiently slowly as to stay in K isotopic equilibrium with the gas. The evaporation potassium does not move, so when the chondrules cool, they do so in a potassium depleted environment.

4 GENERATING SUB-RESERVOIRS

To enrich or deplete the eventual solids in a region of the solar nebula in a moderately volatile element such as K, that element needs to move relative to the "bulk" less volatile elements. The bulk elements can be well represented by Si or Mg, which have similar volatility (50% condensation temperatures of order 1400 K), and which each provide approximately 20% of the non-oxygen mass of a chondrule (Lodders 2003). Note that because we are interested in the K/Si or K/Mg ratios, moving potassium out of a region is equivalent to moving Si and Mg into that region, and vice-versa. At this stage we do not need to know the source of the drift speed, but only its strength. We sketch a cartoon of this process in Figure 1. In it, we show a chondrite assembly region of CI composition. A subsection of it heats to make chondrules, which then drift out of the heating area slowly, leaving the evaporated potassium behind. When they finally cool, they do so in a region with only a small amount of potassium, so only a small amount of potassium recondenses into the chondrules. Once that chondrule forming region also cools, most of the evaporated potassium would instead recondense onto matrix grains. Because the chondrules and the evaporated potassium stay within the larger chondrite assembly area, complementarity is maintained, and if the drift is slow enough, isotopic equilibration would be maintained.

For simplicity, we assume that the relative motion occurs along a single direction, which we label with the coordinate x. If we assume that one participant (volatile or refractory) is tied to the nebular gas and well mixed, while the other participant has a drift speed $\boldsymbol{v} = v\hat{\boldsymbol{e}}_x$ and experiences a turbulent diffusion $\mathcal{D}$, then a steady state is reached when the drift balances diffusion, i.e., when

$$cv = \mathcal{D}\partial_x c, \tag{1}$$

where c is the concentration (with respect to the nebular gas) of the mobile element. Solving Equation (1) we find

$$c = c_0 e^{vx/\mathcal{D}}, \tag{2}$$

where c_0 is the concentration at $x = 0$. Equation (2) leads us to define the length scale

$$\ell_c \equiv \mathcal{D}/v. \tag{3}$$

Depletion or enrichment patterns then can be generated only on length scales $L > \ell_c$. Diffusion is extremely effective at erasing small scale structures so large drift velocities are required to maintain small scale structures, while large scale structures are easier to preserve in the face of diffusion.

However, steady states are not achieved instantly, and it will take a time $t_{\rm gen}$ of order

$$t_{\rm gen} = L/v > \ell_c/v \tag{4}$$

to generate the depletions or enrichments: while large scale structures can achieve significant concentration differences with only moderate drift speeds, those concentration differences require a long time to set up.

To make contact with standard disk theory we scale

$$v = \beta c_s \tag{5}$$

and

$$\mathcal{D} = \alpha c_s H \tag{6}$$

where c_s is the gas background sound speed, β measures v in terms of c_s, α is the Shakura-Sunyaev α parameter (Shakura & Sunyaev 1973), $H = c_s/\Omega_K$ the gas scale height, and Ω_K is the Keplerian frequency. Note that we will use c_s to refer to the background disk sound speeds; and u_{th} for the gas thermal speed in the potassium condensation regions: the existence of cold matrix implies that most of the solar nebula remained cold, well below K condensation temperatures so chondrule forming regions are expected to contain only a small fraction of the total volume (Hubbard & Ebel 2015).

With those scalings, we have

$$\frac{t_{\rm gen}}{\rm Orb} = \frac{\mathcal{D}}{v^2 {\rm Orb}} = \frac{\alpha}{2\pi\beta^2}, \tag{7}$$

where Orb $\equiv 2\pi/\Omega_K$ is the local orbital period. Note that α disks with turbulence driven by orbital shear assume turbulent speeds of order

$$u_t \sim \sqrt{\alpha} c_s. \tag{8}$$

If the drift speed is due to turbulence, we would expect $v \lesssim u_t$ and so $\beta \lesssim \sqrt{\alpha}$ and $t_{\rm gen}/{\rm Orb} \gtrsim 1/2\pi$.

We plot Equation (7) in Figure 2, showing curves of $t_{\rm gen} = 10^{-2}, 1, 100$ orbits. We use $\alpha = 10^{-6}$ as a lower cut-off for the turbulent diffusion because even very laminar disks are expected to be somewhat turbulent and said turbulence will propagate from the turbulent surface layers to the midplane (Oishi & Mac Low 2009). Note that to manage $t_{\rm gen} < 100\,{\rm Orb}$ for $\alpha = 10^{-6}$ we require $\beta > 4 \times 10^{-5}$.

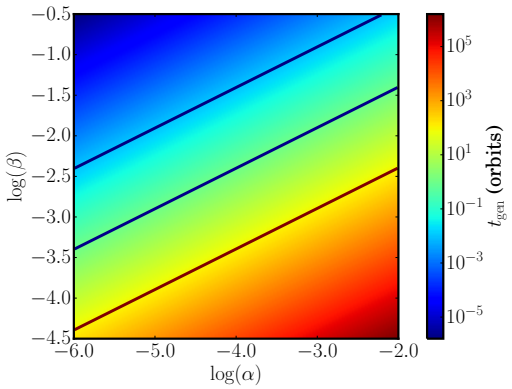

Figure 2. Timescale $t_{\rm gen}$ in orbits as a function of α and β (Equation 7). From top to bottom the lines are $t_{\rm gen} = 10^{-2}, 1, 100\,{\rm Orb}$.

5 DRIFT SPEEDS

As discussed in Section 3, the different reservoirs that produced Type I and II chondrules respectively must have existed within the already different reservoirs that produced the different chondrite classes. To avoid a fine tuning problem we have adopted the assumption that chondrule formation itself naturally produced sub-reservoirs with differing levels of potassium. This process must occurred slowly enough that K isotopic equilibration between gas and dust was continuously maintained. We will also assume elemental equilibration between gas and solids, i.e. that the composition of the solids is only a function of the total (gas and solids) composition and the temperature. This assumption only applies during chondrule formation and any subsequent thermal processing; and is relaxed for temperatures well below 1000 K, when equilibration would take such long time scales that compositions can be considered frozen.

Generating such sub-reservoirs required moving K with respect to Si and Mg, without moving potassium isotopes with respect to one another. The mobile element(s) could have been in the solid or gas phase. If all the elements were in the solid phase, this requires both that there existed categories of dust rich in and depleted in potassium, and that these categories of dust had different aerodynamical properties. We neglect that possibility because this merely pushes the sub-reservoir problem back to the dust growth stage. Note that a 0.25 mm (Friedrich et al. 2015) chondrule made from 0.1 μm interstellar grains would contain the record of 15×10^9 of them, while chondrule precursors would have have K mass fractions of order 5×10^{-4} (Lodders 2003). This means that K is far too abundant for nugget effects to explain its abundances variations between chondrule sized samples.

In what follows we will assume a Hayashi Minimum Mass Solar Nebula (MMSN, Hayashi 1981) normalized to $R = 2.5$ AU, the location of the asteroid belt:

$$T_g \simeq 177 \tilde{R}^{-1/2} {\rm K}, \tag{9}$$

$$c_s \simeq 8 \times 10^4 \tilde{R}^{-1/4}\ {\rm cm\ s^{-1}}, \tag{10}$$

$$\Omega_K \simeq 5 \times 10^{-8} \tilde{R}^{-3/2} {\rm s^{-1}}, \tag{11}$$

$$\Sigma_g \simeq 430 \tilde{R}^{-3/2}\ {\rm g\ cm^{-2}}, \tag{12}$$

$$\rho_0 \simeq 10^{-10} \tilde{R}^{-11/4}\ {\rm g\ cm^{-3}}, \tag{13}$$

where $\tilde{R} \equiv R/2.5$ AU. Unless otherwise specified, we will assume

that the local (hot) gas had a temperature $T_g = 1000\,\mathrm{K}$ with associated thermal speed

$$u_{th} = \sqrt{\frac{2k_B T}{m}} \simeq 2.7 \times 10^5\ \mathrm{cm\ s^{-1}}, \tag{14}$$

where

$$m = \mu m_H \tag{15}$$

was the mean molecular mass of the gas ($\mu \simeq 2.33$). Combining Equations (10) and (14), we find

$$u_{th}/c_s \simeq 3\tilde{R}^{1/4}. \tag{16}$$

Because we are interested only in the potassium signal, and can take chondrule formation as a laboratory given, the details of the dust dynamics prior to chondrule formation, and the details of the chondrule formation scenarios themselves are not vital. Different chondrule formation scenarios naturally allow for different drift speeds, and requirements on t_{gen} will limit the space of viable chondrule formation scenarios.

5.1 Gas motion

If two species were in the gas phase, then for one to have moved with respect to another at meaningful speeds there needs to have existed a force acting differently on two species. An atom of a given species i of mass m_i will encounter its own mass in other atoms in a time

$$t_i = \frac{m_i}{n\sigma u_{th} m}, \tag{17}$$

where

$$n = \frac{\rho_g}{\mu m_H}, \tag{18}$$

is number density of the gas and σ is the effective collisional cross-section.

A force density f exerted on species i (and only on species i) would then drive a drift velocity

$$u_i \sim \frac{f}{\rho_i} \times t_i \simeq \frac{f m_i}{\rho_i \rho_g \sigma u_{th}}. \tag{19}$$

Most forces in protoplanetary disks act on the bulk fluid (e.g. thermal pressure and gravity), and would only drive drift due to smaller differential velocities between different species with differing masses and collisional cross-sections. However, magnetic pressure offers a possible force f which could act on potassium differently than on Mg or Si.

Neutral particle do not feel magnetic forces, so magnetic pressure acts on the disk's gas by exerting a force on charged ions which in turn collide with the mostly neutral gas. Because the ion/neutral coupling is not quite perfect, the ions undergo a slow ambipolar drift through the gas according to Equation (19). Chondrule forming regions are hot enough to thermally ionize potassium. If K^+ is the dominant ion, then the potassium will experience that drift. Note however that type I and II chondrules also differ in their sodium abundances, and sodium is significantly harder to thermally ionize than potassium, and so would drift less.

We can place limits on f by comparing it to

$$f_1 \equiv \frac{\rho_g c_s^2}{H}, \tag{20}$$

the force density required to maintain a 100% bulk gas density variation over a local gas scale height. For $f = f_1$, we find

$$u_i \simeq \frac{m_i \Omega_K}{\rho_i \sigma} \frac{c_s}{u_{th}}. \tag{21}$$

In that case, and for $\sigma \gtrsim 10^{-14}\,\mathrm{cm^2}$ and $\rho_K/\rho_g \simeq 4 \times 10^{-6}$, we have

$$v_K \simeq 0.3\,\mathrm{cm\ s^{-1}}, \tag{22}$$

which corresponds to

$$\beta \simeq 3 \times 10^{-6} \tilde{R}^{1/4}. \tag{23}$$

That value for β is too low to be included on Figure 2, and thanks to the weak radial dependence requires $t_{\mathrm{gen}} \gg 100$ Orb at any orbital position for which the MMSN model applies.

Even in the presence of an extreme magnetic pressure force, and with only extremely weak turbulence, generating elemental abundance differences purely in the gas phase requires many century-scale times. In practice magnetic pressures are lower than assumed in this calculation, and other ions also bear part of the burden (which is important because if K is the only species providing ions, then only the K abundances would be altered through ambipolar drift), both of which would act to reduce v_K and increase t_{gen} even further.

5.2 Dust motion

At temperatures between about $1400\,\mathrm{K} > T > 1000\,\mathrm{K}$, where potassium is partially or fully in the gas phase while Si and Mg are fully condensed, moving the solids through the gas will alter the K/Si and K/Mg ratios. The motion will not inherently generate an isotopic signature because the motion of a dust grain does not meaningfully depend on the difference between even a significant fraction of ^{39}K or ^{41}K atoms. However, if the gas and dust are not in isotopic equilibrium, then dust motion will transport one isotope preferentially. We must therefore assume long enough time scales for the solid motion that equilibration between gas and dust occurs continuously (for a similar process, see Hubbard & Ebel 2014). Further, to reproduce the degree of potassium depletion seen in Type I chondrules ($\sim 80\%$, Hewins 1991), the temperature must have been elevated enough for K to have mostly evaporated while the dust was in motion with respect to the gas.

5.2.1 Settling

Dust embedded in gas tends to drift towards pressure maxima (Weidenschilling 1977). The strongest non-transient pressure gradient in a protoplanetary disk is the vertical one: residual gravity pulls gas and dust towards the midplane, and while a vertical pressure gradient can maintain the gas in hydrostatic equilibrium, the dust does not feel the pressure forces and settles downwards. Other pressure maxima exist in disks, such as zonal flows (Dittrich et al. 2013), although their strength is comparatively limited and they are not expected to last for the entire disk life time. As such, barring extreme examples which are unlikely to have been correlated with chondrule formation (perhaps a radial gap opened by a planet, Zhu et al. 2012), settling can be taken as the strongest drift speed due to gas pressure gradients.

Dust motion through gas is controlled by drag. The equation of motion for dust is

$$\partial_t \boldsymbol{v}_d = -\frac{\boldsymbol{v}_d - \boldsymbol{u}_g}{\tau_d} + \boldsymbol{g} + \cdots, \tag{24}$$

where $\boldsymbol{v}_d$ is the dust velocity, $\boldsymbol{u}_g$ the gas velocity at the dust grain's position, $\boldsymbol{g}$ the gravitational acceleration and τ_d the drag time.

Chondrules have radii significantly smaller than the expected gas molecular mean free path (tens of centimeters for $\rho_g = 10^{-10}$g cm^{-3}), which places them in the Epstein drag regime, with

$$\tau_d = \frac{a\rho_d}{u_{th}\rho_g}, \tag{25}$$

where a and ρ_d are the dust grain radius and solid density, and u_{th} is the actual local gas thermal speed rather than the background disk sound speed c_s. We non-dimensionalize τ_d through

$$\mathrm{St} \equiv \tau_d \Omega_K, \tag{26}$$

the dust Stokes number.

Noting that for a gas disk in vertical hydrostatic equilibrium

$$\rho_g = \rho_0 e^{-z^2/2H^2}, \tag{27}$$

$$\rho_0 = \frac{\Sigma_g}{\sqrt{2\pi}H}, \tag{28}$$

where ρ_0 is the midplane gas density, we can write

$$\mathrm{St} = \tau_d \Omega_K = \left(\frac{c_s}{u_{th}} e^{z^2/2H^2}\right) \mathrm{St}_0, \tag{29}$$

where

$$\mathrm{St}_0 \equiv \frac{a\rho_d}{c_s\rho_0} = \frac{\sqrt{2\pi}a\rho_d}{\Sigma_g} \tag{30}$$

is the dust Stokes number at the midplane. Combining Equations (12) and (30) we find that an $a = 0.25$ mm, $\rho_d = 3\,\mathrm{g\,cm^{-3}}$ chondrule would have had

$$\mathrm{St}_0 = 4 \times 10^{-4} \tilde{R}^{3/2}. \tag{31}$$

For a dust grain of radius a at constant mass m_d,

$$a = \left(\frac{3m_d}{4\pi\rho_d}\right)^{1/3} \propto \rho_d^{-1/3}. \tag{32}$$

From Equation (25) we can see that at constant mass then,

$$\mathrm{St} \propto a\rho_d \propto \rho_d^{2/3}, \tag{33}$$

and note that more porous particles are better coupled to the gas. The porosity of collisionally grown aggregates is as yet uncertain, but in the absence of thermal processing is certainly significant $(80 - 95\%)$ (Zsom et al. 2010) and if compaction is inefficient, could be almost arbitrarily close to unity (Wada et al. 2008).

From Equation (31), we can see that chondrule-sized grains are small enough that terminal velocity can be assumed:

$$v_d = |g\tau_d|. \tag{34}$$

The vertical force of gravity in disks is

$$g_z = -z\Omega_K^2, \tag{35}$$

which results in a settling speed

$$v_s = \mathrm{St}\, z\, \Omega_K, \tag{36}$$

Using $H = c_s/\Omega_K$ and Equation (29) we arrive at

$$\beta \equiv \frac{v_s}{c_s} = \mathrm{St}\frac{z}{H} = \left(\mathrm{St}_0 \frac{c_s}{u_{th}}\right)\left(\frac{z}{H} e^{z^2/2H^2}\right). \tag{37}$$

Equations (33) and (37) show how chondrule formation events would be correlated with settling: thermal processing of high porosity dust leads to compaction, reducing drag, and raising St (Hubbard & Ebel 2014).

Estimating

$$\mathrm{St}_0 \frac{c_s}{u_{th}} \simeq 1.5 \times 10^{-4} \tilde{R}^{5/4}, \tag{38}$$

we can use Equations (7) and (37) to calculate t_{gen} as a function of z/H and α as shown in Figure 3 for $R = 1, 2.5$, and 5 AU. As might be expected, the lower gas densities at larger orbital positions leads to settling being faster. While t_{gen} could be less than 0.01 Orb for low levels of turbulence at modest altitude, such weak turbulence would be unable to strongly loft the chondrule precursors. Takeuchi & Lin (2002) found that the maximum height h to which turbulence will loft grains is approximately

$$\frac{h}{H} = \sqrt{2\ln\left(1 + \frac{\alpha}{\mathrm{St}}\right)}. \tag{39}$$

Chondrule precursor grains with initial porosities of $97, 99.9\%$ would have had $\mathrm{St}_{\mathrm{prec}} = 0.1, 0.01\,\mathrm{St}_0$. The dotted and dashed lines in Figure 3 show the maximum height to which such precursors grains could have been lofted.

In this scenario, values of $t_{\mathrm{gen}} < 0.01$ Orb were therefore possible only for extremely porous precursor grains (porosities above 99.9%) at very high altitudes ($z/H > 3$) at significant ($R > 2.5$ AU) orbital positions, although the altitude and porosity constraints would relax for very large R. Even values of $t_{\mathrm{gen}} = 1$ Orb still require highly ($\sim 97\%$) porous grains and high ($z/H \sim 2.5$) altitudes at $R = 2.5$ AU although again, those constraints are somewhat relaxed by $R = 5$ AU. Note that only about 1.25% of the gas mass was at heights above $z = 2.5$H, and even less of the partially settled, dust mass, so chondrule formation would need to have been quite efficient if restricted to that altitude.

While Figure 3 shows that settling is more effective at larger orbital positions, it measure t_{gen} in units of the local orbit, which also increases with R. While measuring t_{gen} in orbits is useful for comparisons to disk dynamical (e.g. turbulent) time scales, it is less useful for comparison to chemical time scales. For those purposes, we invoke Equation (38) to write

$$t_{\mathrm{gen}} = \frac{\alpha}{\beta^2\Omega_K} \propto \tilde{R}^{-1}, \tag{40}$$

so for settling, larger R is associated with shorter absolute time scales as well.

5.2.2 *Photophoresis*

Photophoresis is a process in which differences in the illumination on two sides of a dust grain generates and maintains a temperature gradient through the grain (Ehrenhaft 1918). As a result, gas molecules rebound faster from the hot side than the cold side, creating a net force that pushes the dust towards its cold side. Photophoresis depends strongly on the details of dust grains' internal thermal conduction. While that can become extremely involved for porous grains (Matthews et al. 2016), chondrule forming regions were by definition hot enough to melt the dust, leaving only comparatively simple solid silicate spheres.

To trap their heat, chondrule forming regions were presumably optically thick, and unable to feel stellar irradiation. However, they were also hot enough to generate their own strong radiation fields that could have driven photophoresis. Recently McNally & Hubbard (2015) derived the photophoretic velocity in the optically thick limit, finding that for solid chondrules with thermal diffusivity $k \simeq 1.5 \times 10^5$ erg s^{-1} cm^{-1} K^{-1},

$$v_p \simeq 2.28 \times 10^{-8} \Gamma \left(\frac{T}{\mathrm{K}}\right)^{7/2} \mathrm{cm\ s^{-1}}, \tag{41}$$

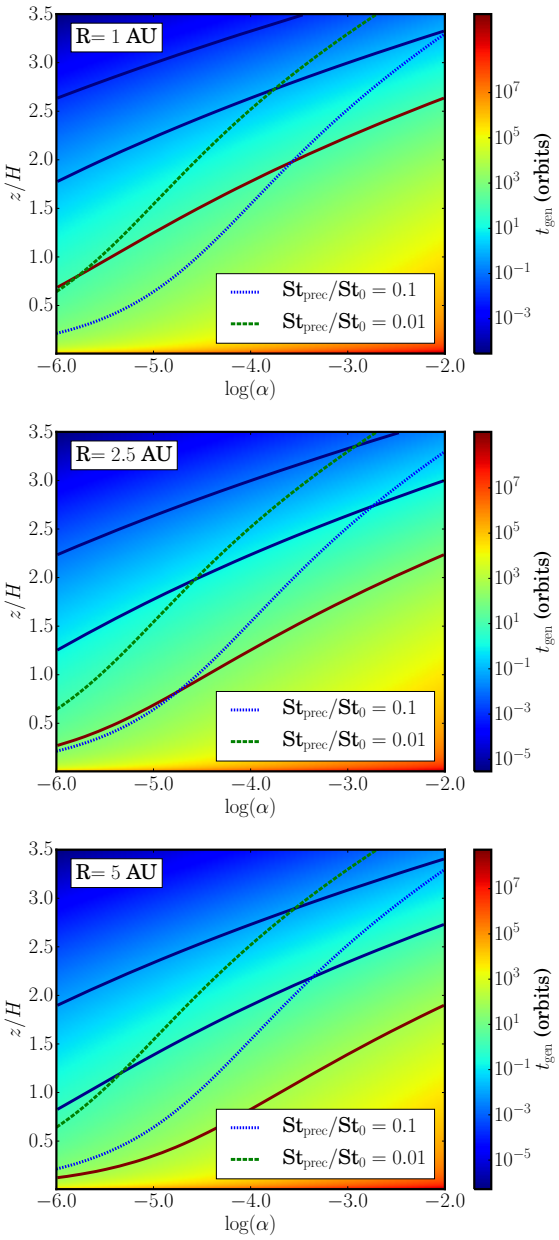

Figure 3. Timescale t_{gen} in local orbits assuming that v is due to settling, for $R = 1, 2.5$, and 5 AU as a function of z/H. From top to bottom the solid lines are $t_{gen} = 10^{-2}, 1, 100$ Orb. The dotted and dashed lines are the highest altitude to which turbulence will mix dust with $St_{prec} = 0.1, 0.01$ St$_0$, respectively.

where κ_R is the Rosseland mean opacity and

$$\Gamma \equiv -\frac{1}{\kappa_R \rho_g}\frac{\partial \ln T_g}{\partial z} \tag{42}$$

measures the temperature gradient in units of optical depths. McNally et al. (2014) found $\Gamma \sim 10^{-4} - 10^{-3}$ for MRI turbulence, although those models assumed a temperature independent opacity and larger values could easily occur under more realistic assumptions, and could have driven much larger values of v_p.

In Figure 4 we show the time scale t_{gen} as a function of α and Γ for $T_g = 1000, 1500$ K at $R = 2.5$ AU. Values of

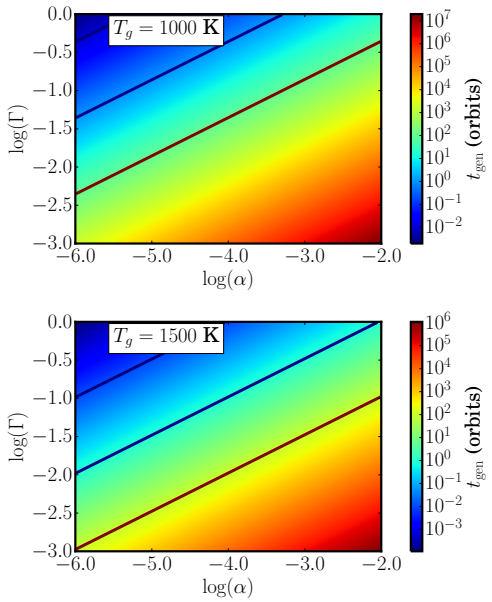

Figure 4. Timescale t_{gen} in orbits at $R = 2.5$ AU, assuming that v is due to photophoresis, for $a = 0.25$ mm fused silica grains. Top panel: $T_g = 1000$ K. Bottom panel: $T_g = 1500$ K. From top to bottom the solid lines are $t_{gen} = 10^{-2}, 1, 100$ Orb.

$t_{gen} < 0.01$ Orb were possible only for extremely large ($\Gamma > 0.1$) temperature gradients combined with the weakest turbulence we consider ($\alpha \sim 10^{-6}$). Values of $t_{gen} = 1$ Orb are more plausible, but still required significantly larger values of Γ than have been seen to date combined with extremely laminar disks. In Equation (41), T is due to the chondrule forming event, rather than the background disk temperature, so v_p is independent of orbital position. From Equation (7), we therefore have

$$\frac{t_{gen}}{\text{Orb}} \propto c_s^2 \propto \tilde{R}^{-1/2}, \tag{43}$$

and

$$t_{gen} \propto \tilde{R}. \tag{44}$$

In terms of dynamical time scales, photophoresis is more effective at larger R, but in terms of absolute time scales, it is more effective at smaller R. Neither of the dependencies is strong enough to alter the above conclusions for reasonable ranges of R.

5.2.3 *Turbulent thermal diffusion*

Turbulent thermal diffusion (TTD) is a process where turbulence preferentially transports moderately well coupled dust grains down gas temperature gradients (from hot to cold) (Elperin et al. 1996). A quick reading of Hubbard (2015b) would suggest that the regions we are considering are warm enough that thermal relaxation would halt the TTD: if turbulent eddies rapidly thermally equilibrate with their surroundings the effects of the temperature gradient are reduced. However, regions associated with chondrule formation are often quite rarified. A $R = 2.5$ AU MMSN midplane at 177 K would have a gas density of $\rho_g = 10^{-10}$ g cm^{-3}, and higher temperature or altitude regions would be expected to be even less dense. Further, during chondrule formation we expect nebular fines to evaporate, and large grains to compactify, resulting in relatively

poor gas-dust thermal coupling, and the gas-dust thermal coupling time can dominate over turbulent time scales.

In high temperature regions, without ices, the gas-to-dust ratio for a mixture of nebular composition is approximately 200 (Lodders 2003). Accordingly, a single grain of mass m_d mediates the radiative thermal relaxation for a parcel of gas of mass $200 m_d$. A temperature perturbation of $\triangle T$ for that parcel corresponds to a thermal energy perturbation of

$$\triangle e = 200 m_d \times \frac{k_B T}{(\gamma - 1)\, m}, \tag{45}$$

where $\gamma \sim 1.4$ is the adiabatic index. Even if the dust temperature is set by radiative equilibrium with the surroundings, the gas will take a time

$$t_{th} = \frac{\triangle e}{4\pi a^2 u_{th} \rho_g \alpha_{\rm tac} \frac{k_B T}{(\gamma-1)m}} \tag{46}$$

to thermally equilibrate with the dust, where the factor of $4\pi a^2 u_{th} \rho_g$ is rate at which gas impinges on the dust grain, and $\alpha_{\rm tac}$ is the thermal accommodation coefficient. Equation (46) can be expanded to find

$$t_{th} \simeq 2 \times 10^5 \left(\frac{u_{th}}{2.7 \times 10^5 \frac{\rm cm}{\rm s}} \right)^{-1} \left(\frac{\rho_g}{10^{-10} \frac{\rm g}{\rm cm}} \right)^{-1} {\rm s}. \tag{47}$$

This implies

$$t_{th} \Omega_K \simeq 10^{-2} \tilde{R}^{5/4}. \tag{48}$$

From appendix A6 of (Hubbard 2015b), the turbulent thermal diffusion velocity is

$$v_{\rm TTD} \simeq -\frac{8}{9} C \tau_s \frac{k_B T}{m} \ln \frac{k_1}{k_2} \partial_z T, \tag{49}$$

where k_1 and k_2 are the limiting wavenumbers of the turbulence which contributes to the TTD, and $C \simeq 0.3$ is a constant of order unity. The upper limit, k_1 is set by the stopping time of the dust grains: turbulent motions with shorter correlation times than the dust stopping time do not contribute. The thermal relaxation time sets the lower limit k_2: turbulent motion with correlation times longer than the thermal relaxation time do not contribute. For a Kolmogorov cascade, the wavenumber scales with the turbulent correlation time as

$$k \propto t^{-3/2}, \tag{50}$$

so Equation (49) becomes

$$v_{\rm TTD} \simeq -\frac{4}{3} C \tau_s \frac{k_B T}{m} \ln \frac{t_{th}}{\tau_s} \partial_z T. \tag{51}$$

We can estimate

$$\ln \frac{t_{th}}{\tau_s} \simeq 3 \tag{52}$$

using Equations (31) and (48).

If we further assume that the temperature gradient was comparable to the local scale height, then $|\boldsymbol{\nabla} \ln T_g| = H^{-1}$, and at $R = 2.5\,{\rm AU}$,

$$v_{\rm TTD} \sim 216\ {\rm cm\ s^{-1}}, \tag{53}$$

which corresponds to

$$\beta = 2.7 \times 10^{-3}. \tag{54}$$

That value of β would have been sufficient to allow for short $t_{\rm gen} < 1\,{\rm Orb}$ for weak, $\alpha < 5 \times 10^{-5}$, turbulence. However, Equation (49) does not apply when $v_{\rm TTD}$ would be comparable to the turbulent speed u_t at the length scale k_0. Assuming that the largest scale turbulence has a velocity scale $\sqrt{\alpha} c_s$ and a time scale Ω_K^{-1}, we have

$$u_t(k_0) \simeq \sqrt{\alpha} c_s k_2^{-1/3} \simeq \sqrt{\alpha t_{th} \Omega_K} c_s. \tag{55}$$

We therefore have the further constraint that $v_{\rm TTD} < \sqrt{\alpha t_{th} \Omega_K} c_s$, which implies $\beta < \sqrt{\alpha t_{th} \Omega_K}$ and hence

$$\frac{t_{\rm gen}}{\rm Orb} \gtrsim \frac{\alpha}{2\pi \left(\alpha t_{th} \Omega_K\right)} \simeq 16 \tilde{R}^{-5/4}, \tag{56}$$

and

$$t_{\rm gen} \propto \tilde{R}^{1/4}. \tag{57}$$

6 COMPARISON TO COOLING CONSTRAINTS

As shown in Section 5, for reasonable ranges of R, values of $t_{\rm gen} < 0.01\,{\rm Orb}$ were only achievable through settling, and even then, only if chondrule formation were limited to extreme altitudes ($z/H > 3$) and chondrule precursors were extremely porous (less than 10^{-3} volume filling fraction). Values of $t_{\rm gen}$ on the order of an orbit was possible through settling at more reasonable, if still high altitudes ($z/H > 2.5$) and for significantly more compacted precursors (97% porosities). At the midplane, turbulent thermal diffusion can drive $t_{\rm gen} \sim 20\,{\rm Orb}$, but significantly smaller values are not expected except for very small R. On the other hand, we do not expect hot thermal structures in the disk to have been extremely long lived, so $t_{\rm gen} < 100\,{\rm Orb}$ would seem a reasonable upper limit.

Accordingly, generating chondrules with significant potassium depletion through evaporation required timescales

$$0.01\,{\rm Orb} < t_{\rm gen} < 100\,{\rm Orb}. \tag{58}$$

If those time scales were not available or are otherwise ruled out, the origin of the potassium abundance variation between chondrules becomes a significant logistical problem. While the details do depend on the orbital position, the dependencies are not extreme, and these conclusions easily hold for $1\,{\rm AU} < R < 5\,{\rm AU}$.

6.1 Chondrule cooling times

These time scales required in Equation (58) are in significant tension with laboratory chondrule cooling constraints. While the experimental limits on chondrule cooling rates vary significantly: $10 - 1000\,{\rm K/hr}$ (Desch et al. 2012, and references therein). Even a very low rate of $10\,{\rm K/hr}$ would cool from 1700 K to 1000 K in under three days, approximately $t_{\rm cool} \lesssim 2 \times 10^{-3}\,{\rm Orb}$ at $R = 2.5\,{\rm AU}$; and the upper end of the cooling rate are far faster, with corresponding far shorter $t_{\rm cool}$. The laboratory constrained cooling time scales put upper limits on the cooling time which are far too short to have allowed particles time to move through the gas and set up potassium abundance variations (i.e. $t_{\rm gen} > 0.01\,{\rm Orb} \gg t_{\rm cool}$).

However, these cooling times $t_{\rm cool}$ are not strictly incompatible with $t_{\rm gen} \gg t_{\rm cool}$ because the cooling rate limits primarily measure thermal histories at crystallization temperatures well above the K condensation temperature which constrains $t_{\rm gen}$. The two constraints can be simultaneously satisfied if the chondrules cooled rapidly through their liquidus temperatures ($T \gtrsim 1400\,{\rm K}$, Hewins & Radomsky 1990), matching observed crystallization patterns; but

then lingered for orbital time scales at K recondensation temperatures ($\sim$ 1000 K) allowing the chondrules to move sufficiently through the gas to generate the observed potassium abundance variations.

7 ISOTOPIC EQUILIBRIUM AND ZONING

A further constraint comes from the lack of a potassium isotopic signature. In the above analysis leading to Equation (58) we have only calculated the time scale required to move chondrules to low potassium regions while the K is entirely evaporated. This means that we have assumed that $\tilde{P}_K \ll P_{K,sat}$, where $\tilde{P}_K$ is potassium's partial pressure were it entirely in the gas phase, and $P_{K,sat}$ its saturation vapor pressure. However, when the potassium recondensed the system moved to the opposite limit, with $\tilde{P}_K \gg P_{K,sat}$. This transition was presumably due to cooling, either because the chondrules moved to regions of lower ambient temperature, or the entire region cooled.

Note that once K began to recondense, the chondrules contributed to the net transport of potassium; and it is imaginable that, were they to have drifted sufficiently rapidly through the gas, they could have entered a region where K would evaporate. We will therefore assume that, especially given the long $t_{\rm gen}$ we predict, the chondrules drifted sufficiently slowly that the system only experienced condensation, i.e. that at all time $P_K \geq P_{K,sat}$, where P_K is K's actual partial partial pressure.

We can follow the results of Richter (2004), invoking a thermal time scale t_T which measures the time for the chondrules to have cooled from being just cool enough for meaningful recondensation to occur to temperatures sufficiently low that complete recondensation can be assumed. We assume that the gas and chondrule fluid densities were high enough that Richter's $\tau_{cond} \ll t_\tau$; and note that Richter's residence time τ_R is conceptually similar to our $t_{\rm gen}$ (although we have the solid, not the gas phase, moving through space). We will also consider the time $t_{\rm diff}$ for K to diffusion through the chondrules near its condensation temperature.

To avoid generating an isotopic signature we need at least one of:

$$t_{\rm diff} \ll t_{\rm gen}, \tag{59}$$

in which case the chondrules were in continuous equilibrium with the gas; or

$$t_T \ll t_{\rm gen} \tag{60}$$

in which case all the available potassium would have recondensed at once, avoiding any isotopic signatures. In this latter case however, if

$$t_T \ll t_{\rm diff}, \tag{61}$$

we would expect the deposition of a potassium layer on the surface of the chondrules, and significant zoning within the chondrules. That is significant because when chondrule precursors melted, they lost potassium proportional to their mass, while when K recondensed it did so at a rate proportional to the surface area: large grains would have become depleted compared to small grains.

7.1 Alkali diffusion times

In general, for element i,

$$t_{{\rm diff},i} = \frac{a^2}{\mathcal{D}_i}, \tag{62}$$

Table 1. Diffusion parameters

Mineral	Na	K
$\mathcal{D}_{\rm rhyolite}$	$\simeq 10^{-6}\,{\rm cm^2\,s^{-1}}$	$\simeq 10^{-8}\,{\rm cm^2\,s^{-1}}$
$t_{\rm diff,\,rhyolite}$	$\simeq 1.2\times10^{3}\,{\rm s}$	$\simeq 6\times10^{4}\,{\rm s}$
$t_{\rm diff,\,rhyolite}$	$\simeq 10^{-5}\tilde{R}^{-3/2}\,{\rm Orb}$	$\simeq 5\times10^{-4}\tilde{R}^{-3/2}\,{\rm Orb}$
$\mathcal{D}_{\rm albite}$	$\simeq 10^{-10}\,{\rm cm^2\,s^{-1}}$	$\simeq 10^{-13}\,{\rm cm^2\,s^{-1}}$
$t_{\rm diff,\,albite}$	$\simeq 7.6\times10^{6}\,{\rm s}$	$\simeq 8\times10^{9}\,{\rm s}$
$t_{\rm diff,\,albite}$	$\simeq 6.4\times10^{-2}\tilde{R}^{-3/2}\,{\rm Orb}$	$\simeq 66\tilde{R}^{-3/2}\,{\rm Orb}$

where $\mathcal{D}_i$ is the appropriate diffusion coefficient for that element. Unfortunately, diffusion coefficient measurements for K and Na through different minerals differ by orders of magnitude depending on the mineral. In Table 1 we list the diffusion coefficients for K and Na in rhyolite and albite (Brady 2013, and references therein), as well as the associated diffusion timescales through $a = 0.25$ mm spheres. We can see that, in general, Na diffuses rapidly and is expected to satisfy $t_{\rm diff} \ll t_{\rm gen}$, but, depending on the minerals involved, K may not.

This means that the lack of Na zoning seen by Alexander et al. (2008) is not unexpected for a locally generated depletion/enhancement of Na (which would be expected to track that of K given their similar volatility): chondrules are expected to internally equilibrate Na on time scales $t_{\rm diff} \ll t_{\rm gen}$. The "a few" orders of magnitude difference between Na and K diffusivities also suggests that any observed difference in K and Na zoning within a given chondrule would, if combined with a detailed internal diffusion model for that chondrule, provide a direct measure for $t_{\rm gen}$: the condensation temperatures for Na and K are sufficiently close that the two elements experienced similar values of $t_{\rm gen}$ and t_T.

8 CONCLUSIONS

The observed strongly varying degrees of potassium depletion between chondrules required the existence of separate reservoirs with different alkali metal abundances. We have explored how such different reservoirs could have been locally created in the solar nebula, concluding that while they might have been straightforwardly produced by heating the gas enough to evaporate the alkalis and subsequently transporting the solids through the gas, leaving the alkalis behind, the time scales required were significant: sub-orbital to hundreds of orbits. Further, the lower end of the time scales are only available if chondrule formation occurred at altitude, and chondrule precursors were very porous. This porosity requirement is problematic because high dust porosities are not expected to survive temperatures $T \sim 1000$ K (far below chondrule processing temperatures): silicate grains are expected to rapidly coalesce at such temperatures, reducing their porosity (Hubbard 2015a). If chondrule formation occurred at the midplane, the minimum time scales balloon to tens of orbits. This is not entirely surprising: chondrules are very small, and hence were very well tied to the gas (Jacquet et al. 2012; Hubbard & Ebel 2015). Moving chondrules through the gas was hence a laborious process.

Such long time scales are in significant tension with laboratory estimates of chondrule cooling rates, which were much faster. That tension would be resolved if newly formed chondrules rapidly cooled enough to lock in their petrology ($T \gtrsim 1400$ K, Hewins & Radomsky 1990), but subsequently stayed warm ($T \gtrsim 1000$ K) for long enough for them to have slipped through the gas. On the

other hand, long timescales could simplify the puzzling lack of Na zoning in chondrules seen by Alexander et al. (2008): if the chondrules stayed warm long enough for Na (and possibly K) to have fully diffused through its host, then there would have been no need for extreme concentrations of solids in chondrule forming regions. Staying at $T \gtrsim 1000\,\mathrm{K}$ for prolonged periods is significant because that temperature is associated with thermal ionization of alkali metals which are significantly evaporated, allowing the MRI to be active (Gammie 1996). This would support the case for MRI turbulent dissipation as a chondrule heating mechanism (Hubbard et al. 2012; McNally et al. 2013, 2014).

If, however, such time scales spent warm were not available, then the origin of the different reservoirs with differing elemental, but not isotopic, abundances becomes a major logistical problem. The lack of a potassium isotopic signature rules out a presolar source for the different reservoirs, and any other model will have to wrestle with the improbabilities associated with generating many reservoirs. That difficulty is compounded by complimentarity, which argues that the reservoirs from which chondrules in a given chondrite formed were correlated. Further, the presence of cold matrix strongly constrains the amount of thermal processing that could have occurred in the solar nebula: most of the solids were never thermally processed enough to evaporate potassium (Hubbard & Ebel 2015), so if the potassium abundance variations were thermal in origin, and were generated in the solar nebula, they must have been correlated with chondrule formation, lest the thermally processed material show up in the matrix.

The long time scales required to have generated potassium abundance variations in the solar nebula can also explain the lack of potassium isotope signatures throughout the Solar System, even between bodies with wildly varying potassium abundances (Humayun & Clayton 1995). Isotopic equilibration is to be expected if, as in the case of chondrules, the time scales required to physically move the solids through gas (which is required to deplete or enhance the potassium abundances) are long compared to K's evaporation or recondensation time scales. Indeed, a potassium isotopic signature would be of great use in determining the time scale of physical processes in the solar nebula.

ACKNOWLEDGEMENTS

The research leading to these results received funding from NASA OSS grant NNX14AJ56G.

REFERENCES

Alexander, C. M. O. . 2004, Geochimica Cosmochimica Acta, 68, 3943
Alexander, C. M. O. ., Grossman, J. N., Ebel, D. S., & Ciesla, F. J. 2008, Science, 320, 1617
Alexander, C. M. O., Grossman, J. N., Wang, J., et al. 2000, Meteoritics and Planetary Science, 35, 859
Alexander, C. M. O., & Wang, J. 2001, Meteoritics and Planetary Science, 36, 419
Bai, X.-N. 2014, ApJ, 791, 137
Boley, A. C., Morris, M. A., & Desch, S. J. 2013, ApJ, 776, 101
Brady, J. B. 2013, Diffusion Data for Silicate Minerals, Glasses, and Liquids (American Geophysical Union), 269
Cuzzi, J. N., Hogan, R. C., Paque, J. M., & Dobrovolskis, A. R. 2001, ApJ, 546, 496
Davis, A. M., Alexander, C. M. O., Nagahara, H., & Richter, F. M. 2005, in Astronomical Society of the Pacific Conference Series, Vol. 341, Chondrites and the Protoplanetary Disk, ed. A. N. Krot, E. R. D. Scott, & B. Reipurth, 432
Desch, S. J., Morris, M. A., Connolly, H. C., & Boss, A. P. 2012, Meteoritics and Planetary Science, 47, 1139
Dittrich, K., Klahr, H., & Johansen, A. 2013, The Astrophysical Journal, 763, 117
Draine, B. T. 2003, ARA&A, 41, 241
Ehrenhaft, F. 1918, Annalen der Physik, 361, 81
Elperin, T., Kleeorin, N., & Rogachevskii, I. 1996, Physical Review Letters, 76, 224
Friedrich, J. M., Weisberg, M. K., Ebel, D. S., et al. 2015, Chemie der Erde - Geochemistry, 75, 419
Gammie, C. F. 1996, ApJ, 457, 355
Goldberg, A. Z., Owen, J. E., & Jacquet, E. 2015, MNRAS, 452, 4054
Hayashi, C. 1981, Progress of Theoretical Physics Supplement, 70, 35
Hewins, R. H. 1991, Geochimica Cosmochimica Acta, 55, 935
Hewins, R. H. 1997, Annual Review of Earth and Planetary Sciences, 25, 61
Hewins, R. H., & Radomsky, P. M. 1990, Meteoritics, 25, 309
Hezel, D. C., & Palme, H. 2010, Earth and Planetary Science Letters, 294, 85
Hubbard, A. 2013, MNRAS, 432, 1274
Hubbard, A. 2015a, Icarus, 254, 56
Hubbard, A. 2015b, ArXiv e-prints, arXiv:1512.02538 [astro-ph.EP]
Hubbard, A., & Ebel, D. S. 2014, Icarus, 237, 84
Hubbard, A., & Ebel, D. S. 2015, Icarus, 245, 32
Hubbard, A., McNally, C. P., & Mac Low, M.-M. 2012, ApJ, 761, 58
Humayun, M., & Clayton, R. N. 1995, Meteoritics, 30, 522
Huss, G. R., & Lewis, R. S. 1995, Geochimica Cosmochimica Acta, 59, 115
Jacquet, E., Gounelle, M., & Fromang, S. 2012, Icarus, 220, 162
Johansen, A., Youdin, A., & Mac Low, M.-M. 2009, ApJ, 704, L75
Jones, R. H. 1990, Geochimica Cosmochimica Acta, 54, 1785
Jones, R. H. 2012, Meteoritics and Planetary Science, 47, 1176
Jones, R. H., & Scott, E. R. D. 1989, in Lunar and Planetary Science Conference Proceedings, Vol. 19, Lunar and Planetary Science Conference Proceedings, ed. G. Ryder & V. L. Sharpton, 523
Lodders, K. 2003, ApJ, 591, 1220
Lynden-Bell, D., & Pringle, J. E. 1974, MNRAS, 168, 603
Matthews, L. S., Kimery, J. B., Wurm, G., et al. 2016, MNRAS, 455, 2582
McDonough, W. F. 2003, Treatise on Geochemistry, 2, 547
McNally, C. P., & Hubbard, A. 2015, ApJ, 814, 37
McNally, C. P., Hubbard, A., Mac Low, M.-M., Ebel, D. S., & D'Alessio, P. 2013, ApJ, 767, L2
McNally, C. P., Hubbard, A., Yang, C.-C., & Mac Low, M.-M. 2014, ApJ, 791, 62
McSween, Jr., H. Y. 1977a, Geochimica Cosmochimica Acta, 41, 477
McSween, Jr., H. Y. 1977b, Geochimica Cosmochimica Acta, 41, 1843
Mendybaev, R. A., Beckett, J. R., Grossman, L., et al. 2002, Geochimica Cosmochimica Acta, 66, 661
Morris, M. A., Boley, A. C., Desch, S. J., & Athanassiadou, T. 2012, ApJ, 752, 27
Oishi, J. S., & Mac Low, M.-M. 2009, ApJ, 704, 1239
Palme, H. 2000, Space Sci. Rev., 92, 237
Palme, H., Hezel, D. C., & Ebel, D. S. 2015, Earth and Planetary Science Letters, 411, 11
Richter, F. M. 2004, Geochimica Cosmochimica Acta, 68, 4971
Shakura, N. I., & Sunyaev, R. A. 1973, A&A, 24, 337
Takeuchi, T., & Lin, D. N. C. 2002, ApJ, 581, 1344
Van Schmus, W. R., & Wood, J. A. 1967, Geochimica Cosmochimica Acta, 31, 747
Wada, K., Tanaka, H., Suyama, T., Kimura, H., & Yamamoto, T. 2008, ApJ, 677, 1296
Weidenschilling, S. J. 1977, MNRAS, 180, 57
Weisberg, M. K., McCoy, T. J., & Krot, A. N. 2006, Systematics and Evaluation of Meteorite Classification, ed. D. S. Lauretta & H. Y. McSween, 19

Yu, Y., & Hewins, R. H. 1997, in Lunar and Planetary Inst. Technical Report, Vol. 28, Lunar and Planetary Science Conference, 1613
Zhu, Z., Nelson, R. P., Dong, R., Espaillat, C., & Hartmann, L. 2012, ApJ, 755, 6
Zsom, A., Ormel, C. W., Güttler, C., Blum, J., & Dullemond, C. P. 2010, A&A, 513, A57